https://doi.org/10.31925/farmacia.2023.6.17 **ORIGINAL ARTICLE**

SYNTHESIS, *IN SILICO* STUDY AND ANTITUMOR ACTIVITY OF COUMARIN COMPOUNDS IN LYMPHOMA CELLS

ESMA BILAJAC [1], AMAR OSMANOVIĆ [2]*, UNA GLAMOČLIJA [2,3,4], ELMA VELJOVIĆ [2], BELMA IMAMOVIĆ [2], ERVINA BEČIĆ [2], SUNČICA ROCA [5], MIRSADA SALIHOVIĆ [2], DAVORKA ZAVRŠNIK [2], SELMA ŠPIRTOVIĆ-HALILOVIĆ [2]

[1]*Department of Genetics and Bioengineering, Faculty of Engineering and Natural Sciences, International University of Sarajevo, Hrasnička cesta 15, 71000 Sarajevo, Bosnia and Herzegovina*
[2]*University of Sarajevo - Faculty of Pharmacy, Zmaja od Bosne 8, 71000 Sarajevo, Bosnia and Herzegovina*
[3]*School of Medicine, University of Mostar, Zrinskog Frankopana 34, 88000 Mostar, Bosnia and Herzegovina*
[4]*Scientific-Research Unit, Bosnalijek JSC, Jukićeva 53, 71000 Sarajevo, Bosnia and Herzegovina*
[5]*NMR Centre, Ruđer Bošković Institute, Bijenička cesta 54, 10000 Zagreb, Croatia*

**corresponding author: amar.osmanovic@ffsa.unsa.ba*

Manuscript received: September 2023

Abstract

Coumarin derivatives are characterised by a wide range of therapeutic applications, including anti-tumour activity. Using in silico and in vitro approaches, we evaluated the possible antitumor effects of four 3-cinnamoyl-4-hydroxycoumarin derivatives in diffuse large B- cell lymphoma (DLBCL) cells.. Also, molecular properties and several ADME parameters were our subjects of investigation. The results of an in silico molecular docking analysis show that coumarin compounds have a strong affinity for binding to Akt, NF-κB and Mcl-1 protein targets, which are important for controlling the growth, differentiation and survival of DLBCL cells. Analysed molecular and ADME properties show that compounds satisfy Lipinski's rule of five. The WST-8 test showed that coumarin derivatives with bromine substituents had a strong cytotoxic effect on HBL-1 cells, which are a type of more aggressive activated B-cell (ABC) DLBCL. However, treatment of DHL-4 germinal centre B-cell (GCB) DLBCL cells with the same substanceshowed no inhibitory activity, suggesting diverse mechanism of action among two distinct DLBCL models.Western blot analysis indicated stimulatory activity of compound 2, with increased Akt phosphorylation levels in both types of cells. These results represent an insight into the activation of the compensatory Akt mechanisms in DLBCL cells. This could represent a key step in combinatorial treatment approaches in order to avoid drug resistance and achieve greater therapeutic efficacy in DLBCL cells.

Rezumat

Derivații cumarinici se caracterizează printr-o gamă largă de acțiuni terapeutice, incluzând activitatea antitumorală. În cadrul acestui studiu, a fost investigată *in silico* și *in vitro* potențiala activitate antitumorală în limfomul difuz cu celule B mari (DLBCL) și descrisă farmacocinetica pentru patru derivați sintetizați de 3-cinamoil-4-hidroxicumarină. Datele analizei *in silico* sugerează afinități puternice de legare a compușilor cumarinici față de țintele proteice Akt, NF-κB și Mcl-1 ca regulatori principali ai proliferării, diferențierii și supraviețuirii celulelor DLBCL. Rezultatele analizei WST-8 au arătat un efect citotoxic puternic al derivatului de cumarină cu substituent de brom în celulele HBL-1 ce aparțin subtipului mai agresiv DLBCL al celulei B activate. Cu toate acestea, în cazul tratării celulelor DLBCL din centrul germinal B (GCB) DHL-4 cu aceeași substanță nu s-a observat nicio activitate inhibitorie, sugerându-se astfel un alt mecanism de acțiune. Analiza Western Blot a demonstrat activitatea stimulatoare a compusului 2, cu niveluri crescute de fosforilare a Akt. Rezultatele studiului oferă o mai bună înțelegere a modului în care funcționează mecanismul compensator Akt în celulele DLBCL. Acesta ar putea fi un pas esențial în găsirea unor noi abordări terapeutice a celulelor DLBCL rezistente la tratament.

Keywords: coumarins, DLBCL, antitumor activity, molecular docking, ADME, molecular properties

Introduction

Cancer represents one of the leading causes of death worldwide, with 19.3 million newly diagnosed cases and approximately 10 million cancer-related deaths in 2020. The expectancy rate of cancer is about to increase to 28.4 million cases in 2040, therefore, cancer remains one of the major health issues world-wide [1]. Among numerous cancer types, diffuse large B-cell lymphoma (DLBCL) is one of the most commonly diagnosed types of non-Hodgkin's lymphoma (NHL), comprising a heterogenous group of neoplasms that differ at molecular and pathological levels [2, 3]. DLBCL represents a significant health problem that affects millions of people worldwide as it accounts for approximately 30 - 40% of the total number of newly diagnosed B-cell NHL cases in different geographical areas [2-4]. Based on gene expression profiling, DLBCL is classified into activated B-cell (ABC) that is present in 40 - 50% of cases, germinal centre B-cell

(GCB) (50 - 60%), as well as a small unclassified group detected in approximately 10% of the patients [5, 6]. The major hallmarks of ABC and GCB DLBCL are the constitutive activation of nuclear factor kappa B (NF-κB) and phosphatidylinositol-3 kinase signalling pathways, respectively, that promote cancer cell survival and proliferation while inhibiting apoptosis [7, 8]. The current treatment options for DLBCL include cyclophosphamide, doxorubicin, vincristine, prednisone, plus the monoclonal antibody rituximab (R-CHOP). However, the common problem in DLBCL treatment is the therapeutic failure present in 30 - 40% of the patients [9]. As the incidence of DLBCL is increasing worldwide, novel therapeutic approaches for disease treatment that result in higher response rates are urgently warranted. This has prompted us to investigate the potential anticancer activity of four 3-cinnamoyl-4-hydroxycoumarin derivatives in DLBCL cells [10, 11], where two compounds represent newly synthesised substances whose structures were not previously reported.

The literature data indicate a wide range of pharmacological activities of coumarins that depend on the core structure and substitution pattern, including antibacterial, antifungal, antiviral, antioxidant, anti-inflammatory, antithrombotic, cytotoxic, antitumor and many others [12-15].

In our previous work, we evaluated the antimicrobial activity of compounds 3-(3-(4-chlorophenyl)prop-2-enoyl)-4-hydroxy-2H-1-benzopyran-2-one (compound 1) and 3-(3-(4-bromophenyl)prop-2-enoyl)-4-hydroxy-2H-1-benzopyran-2-one (compound 2) using diffusion method. The results suggest that both of the compounds inhibit the growth of Gram-positive aerobic bacteria *B. subtilis* and *B. cereus*, with more prominent antimicrobial activity of compound 2 bearing bromine substituent in both models. Density functional theory (DFT) analysis showed that the mentioned substance is the most stable and least reactive compound, probably as a result of lower bromine electronegativity in comparison to chlorine [10, 11]. In addition, compound 2 showed the strongest activity against *S. aureus*, while both of the substances were also effective against *S. aureus* and *B. subtilis* assessed by the dilution method [16].

In this study, we synthesized two novel 3-cinnamoyl-4-hydroxycoumarin derivatives, including 3-(3-(2,5-dimethoxyphenyl)acryloyl)-4-hydroxycoumarin (compound 3) and 3-(3-(2,4,6-trimethoxyphenyl)-acryloyl)-4-hydroxycoumarin (compound 4). The molecular docking method was used to determine the binding affinities of coumarin compounds toward the main protein targets as a main regulators of DLBCL tumorigenesis. Except docking, numerous other molecular and pharmacokinetic parameters, that provide information about the potency of some compounds to become drugs, were investigated *in silico*. The anticancer effects of these compounds had not been reported before, so the goal of this study was to test the antitumor effects of four coumarin compounds in ABC and GCB DLBCL models.

Materials and Methods

The synthesis and structure elucidation of 3-cinnamoyl-4-hydroxycoumarins

The synthesis and structure elucidation process of 3-cinnamoyl-4-hydroxycoumarins was previously reported [17, 18].

Prediction of molecular and ADME descriptors

Lipophilicity (iLOGP) [19], number of hydrogen bond donors (HBD) and acceptors (HBA), molecular weight (MW), topological polar surface area (TPSA), molar refractivity (MR) and number of rotatable bonds (nRotb) were calculated using the SwissADME online tool (http://swissadme.ch/) [20]. Various ADME properties (CaCo-2 cell permeability, human intestinal absorption, plasma protein binding, blood-brain barrier penetration, skin permeability and Maden Darby canine kidney cell permeability) of the synthesized compounds were predicted using the preADMET online server (http://preadmet.bmdrc.org/).

Molecular docking analysis

The molecular docking study was set up in YASARA Structure 23.9.29 software [21, 22] and performed using AutoDock 4.2 [23]. The crystal structures of NF-kB p52/RelB/DNA complex (PDB ID: 3DO7), protein kinase B/Akt (PDB ID: 1GZO) and MCL-1 (PDB ID: 6B4L) were downloaded from the RCSB Protein Data Bank (www.rcsb.org/) and used as target molecules. The structures of protein targets were prepared by removing water molecules, adding polar hydrogen atoms and optimizing in the AMBER03 force field [24]. The 3D structures of the coumarin molecules were prepared and geometries were optimized by the MM2 force field [25, 26] using PerkinElmer Chem3D Ultra 16.0.1.4. software. Molecular docking analyses were performed using either the blind docking method or setting up the search area box around a specific binding pocket. The Lamarckian genetic algorithm was employed with the following parameters: 10 docking runs with a maximum of 15,000,000 energy evaluations and 27,000 generations for each run, with a grid point spacing of 0.375 Å, providing this way the lowest energy docked poses.

Cell culture and substance preparation

HBL-1, DHL-4 and MRC-5 cell lines were cultured in Roswell Park Memorial Institute (RPMI)-1640 basal medium (Sigma Aldrich, USA) supplemented with 10% Foetal Bovine Serum (FBS), 100 U/mL penicillin, 100 μ/mL streptomycin, 10 mM HEPES, 1 mM sodium pyruvate and 1% of non-essential amino acid α-glutamine (Sigma Aldrich, USA). HBL-1 is a diffuse large B-cell lymphoma carrying 14q32 translocation and it is assigned to ABC lymphoma subtype and B-cell receptor DLBCL [27]. DHL-4 is a

B-cell lymphoma cell line assigned to GCB lymphoma subtype and B-cell receptor DLBCL [27]. Cell cultures were grown in suspension and maintained at optimal conditions in a humidified atmosphere (95%), 5% CO_2 at 37°C. The compounds were dissolved in 100% DMSO (Sigma-Aldrich, UK) as a stock solution of 100 mM concentration and further diluted in 1x phosphate-buffered saline (PBS) (Fisher Bioreagents, USA). Compound **3** was not soluble in PBS or DMSO and it was excluded from biological assays.

Cell viability assay

Cell viability was determined by the WST-8 assay (Bimake, USA). DLBCL cells were plated in triplicates in a 96-well plate at an optimum seeding density of 2.5 x 10^4 cells/well and treated with 0.10, 10.00 and 50.00 μM compounds' concentrations for 48 hours. MRC-5 lung fibroblast cells were seeded at 1 x 10^4 cells/well seeding density and left to adhere overnight. The cells were treated with 25.00, 50.00 and 100.00 μM compound concentrations. The highest percentage of DMSO in wells treated with compounds was 0.1%. The same percentage of DMSO was used as a negative control. After incubation, a cell viability assay was performed according to the manufacturer's protocol.

Trypan blue assay

Cell death was determined by trypan blue exclusion assay. HBL-1 and DHL-4 cells were treated with different concentrations of compound **2** (0.00, 1.25, 2.50, 5.00, 10.00, 20.00, 40.00 and 50.00 μM) for 48 hours. Cells were mixed and stained with 0.4% filtered trypan blue solution (GibcoTM Life Technologies, Waltham, MA, USA) and counted with Countess II FL Automated Cell Counter (Thermo Fisher Scientific, Waltham, MA, USA). The results are represented as a percentage relative to the negative control (0.05% DMSO) set as 100% of cell viability.

Western blot analysis

For Western blot analysis, cells were spread out in a 6-well plate at a density of 1 x 106 cells/well and treated with compound 2 for 48 hours. As a negative control, cells that were treated with 0.01% DMSO were also used. Cells were lysed in ice-cold RIPA buffer supplemented with protease and phosphatase inhibitors (Sigma-Aldrich, UK). 12% SDS-polyacrylamide gel electrophoresis (SDS-PAGE) was used to separate all the samples, and the separated proteins were then put on a PVDF membrane (Merck Millipore, Germany). The membrane was blocked with 5% BSA in Tris-buffered saline supplemented with 0.1% Tween-20 buffer (Sigma-Aldrich, UK). Western blot analyses were performed using primary antibodies against phospho-NF-κB p65 (Ser536) (93H1) Rabbit mAb #3033, phospho-Akt (Ser473) (D9E) XP® Rabbit mAb #4060 and Mcl-1 (4572) Rabbit antibody. For loading control, β-Actin (8H10D10) Mouse mAb #3700 primary antibody was used. Secondary antibodies anti-rabbit IgG, HRP-linked antibody #7074 and anti-mouse IgG, HRP-linked Antibody #7076 were used (Cell Signaling Technology, USA). The signals were detected using AmershamTM ECLTM Prime Western Blotting Detection Reagent (GE Healthcare Life Sciences, UK). Protein bands were visualized by Molecular Imager ChemiDocTM XRS+ Imaging System (Bio-Rad, USA) and analysed by Image Lab software (v.6.0).

Statistical analysis

GraphPad PRISM software, version 8.3 was used for statistical analysis. The results of different experiments were represented as means ± standard deviation (SD) of three to four independent experiments. The normal distribution of variances was tested by the D'Agostino-Pearson normality test. Shapiro-Wilk test was used where the normality test indicated the normal distribution of variances ($p > 0.05$), whereas Kolmogorov-Smirnov test was used otherwise. One-way ANOVA Dunnett's multiple comparison analysis was used for statistical evaluation. $P < 0.05$ was considered a level of statistical significance with the next levels presented through the text: *$p < 0.05$, **$p < 0.01$, ***$p < 0.001$, ****$p < 0.0001$, ns – not significant.

Results and Discussion

Structure elucidation of novel derivatives

3-(3-(2,5-dimethoxyphenyl)acryloyl)-4-hydroxycoumarin (compound **3**)

Yield: 74%; m.p. 182 - 184°C; UV/Vis (DMSO) λ_{max}/nm: 340.4; IR (KBr) ν (cm^{-1}): 1723 (C=O lactone); 1595, 1489, 1410, (C=C, aromatic); 1338, 1114 (C-O), 1276 (C-O); 879, 812, 745 (C-H, trisubstituted benzene ring); ^{1}H NMR (600 MHz, $CDCl_3$-d): δ 18.83 (1H, br s, OH), 8.38 (1H, d, *J* = 15.48 Hz, H-12), 8.23 (1H, d, *J* = 15.48 Hz, H-13), 8.06 (1H, dd, *J* = 7.95; 1.32 Hz, H-5), 7.84 (1H, dd, *J* = 7.95; 1.32 Hz, H-7), 7.48 - 7.41 (2H, m, H-6 and H-8), 7.24 (1H, d, *J* = 2.16 Hz, H-19), 7.15 - 7.09 (2H, m, H-16 and H-17), 3.88 (3H, s, O$C\underline{H}_3$-15), 3.78 (3H, s, O$C\underline{H}_3$-18) ppm; ^{13}C NMR (150 MHz, $CDCl_3$-d): δ 191.9 (C-11), 180.9 (C-4), 159.5 (C-2), 154.2 (C-9), 153.4 (C-15), 153.2 (C-18), 141.4 (C-13), 136.6 (C-7), 125.4 (C-5), 124.7 (C-6), 123.1 (C-14), 123.0 (C-12), 119.2 (C-17), 116.9 (C-8), 113.6 (C-19), 113.4 (C-16), 100.8 (C-3), 56.2 (O$\underline{C}H_3$-15), 55.6 (O$\underline{C}H_3$-18) ppm; C-10 was not detected.

3-(3-(2,4,6-trimethoxyphenyl)acryloyl)-4-hydroxycoumarin (compound **4**)

Yield: 78%; m.p. 228 - 230°C; UV/Vis (DMSO) λ_{max}/nm: 343.4; IR (KBr) ν (cm^{-1}): 3144 (C-H, unsaturated); 1712 (C=O, lactone), 1595, 1483, 1415 (C=C, aromatic); 1276 (C-O); 807, 756 (*p*-substitution); ^{1}H NMR (600 MHz, $CDCl_3$-d): δ19.26 (1H, br s, OH), 8.63 (1H, d, *J* = 14.90 Hz, H-12), 8.48 (1H, d, *J* = 14.90 Hz, H-13), 8.03 (1H, d, *J* = 7.57 Hz, H-5), 7.80 (1H, t, *J* = 7.31 Hz, H-7), 7.42 (1H, t, *J* = 7.57 Hz, H-6), 7.39 (1H, d, *J* = 8.36 Hz, H-8), 6.34 (2H, s, H-16 and H-18), 3.94 (6H, s, O$C\underline{H}_3$-15/19), 3.90 (3H,

s, OC<u>H</u>$_3$-17) ppm; ^{13}C NMR (150 MHz, $CDCl_3$-d): δ 191.4 (C-11), 182.0 (C-4), 165.1 (C-17), 162.3 (C-15/19), 159.3 (C-2), 154.1 (C-9), 139.0 (C-13), 136.2 (C-7), 125.4 (C-5), 124.4 (C-6), 119.6 (C-12), 116.7 (C-8), 105.7 (C-14), 100.0 (C-3), 91.2 (C-16/18), 56.2 (O<u>C</u>H$_3$-15/19), 55.8 (O<u>C</u>H$_3$-17) ppm; C-10 was not detected.

Predicting the permeability and bioactivity of investigated derivatives

In the initial stages of testing for biologically active compounds, numerous molecular parameters and pharmacokinetic properties are used to provide information about the potency of some compounds to become drugs. The ability of the drug to permeate through the membrane is one of the first parameters tested in the new drug modelling process. Lipinski's rule of five is one well-known set of parameters useful in this process. According to this rule, a molecule will be able to passively permeate through the intestinal membrane if its properties are within the next range: a molecular weight of less than 500 g/mol, a log P value of less than 5 representing its lipophilicity, no more than 5 hydrogen bond donor (HBD) and no more than 10 hydrogen bond acceptor (HBA) sites [28]. Further research has expanded this set by a few more conditions, such as molar refractivity (a measure of the overall polarity of a molecule) ranging from 40 to 130, a topological polar surface area (TPSA) of less than or equal to 140 Å^2 and less than 10 rotatable bonds (RB) [29] which closely describe drug's permeability and flexibility.

Therefore, if the compound follows these rules and parameters, it is expected to be orally bioavailable. If the molecule violates any two or more of the above requirements, it is assumed that it will not be capable to permeate by passive intestinal diffusion. Besides absorption, other pharmacokinetic parameters of a compound can be predicted based on lipophilicity, including distribution, elimination and toxicity.

Oral bioavailability parameters for the test compounds are shown in Table I. All of the compounds were predicted to have good oral bioavailability as their iLOGP values ranged from 2.32 to 3.28, molecular weights were less than 500 g/mol and all of the compounds had only one hydrogen bond donor and less than 10 hydrogen bond acceptors (4 - 7). The rest of the parameters, such as the number of rotatable bonds, MR and TPSA values were within the allowed ranges.

Table I

Molecular properties of tested coumarins

Compound	TPSA (Å^2)	iLOGP	MW (g/mol)	nON	nOHNH	nRotb	MR
1	67.51	2.32	326.73	4	1	3	89.32
2	67.51	2.68	371.18	4	1	3	92.01
3	85.97	3.20	352.34	6	1	5	97.30
4	95.20	3.28	382.36	7	1	6	103.79

iLOGP: lipophilicity; TPSA: topological polar surface area; MW: molecular weight; nON: sum of hydrogen bond acceptors; nOHNH: sum of hydrogen bond donors; nRotb: number of rotatable bonds; MR: molar refractivity

TPSA, measured in Å^2, represents a sum of fragment contributions of O- and N- cantered polar fragments. Synthesized compounds have a different number of oxygen atoms (a different environment) and none of the nitrogen atoms. The largest TPSA was observed for compound **4**. Molecular flexibility is another important parameter in determining the oral bio-availability of the drugs. It is characterized by the number of rotatable bonds (nRotb), which are defined as any single non-ring bond, bound to a nonterminal heavy (*i.e.*, non-hydrogen) atom [30]. According to some authors, the number of rotatable bonds should be ≤ 10, therefore all of the tested compounds used in this study complied with the given recommendation [30].

For all synthesized compounds, three rotatable bonds are observed at the C-3 cinnamoyl side chain of the main coumarin moiety. The additional rotatable bonds of compounds **3** and **4** are between the carbons on the phenyl ring and the oxygens from the methoxy groups (Figure 1).

ADME parameters of tested compounds are shown in Table II.

Table II

ADME parameters of tested coumarins

Compound	Absorption		PPB (%)	BBB (c_{brain}/c_{blood})	SKIN (logKp)	MDCK (nm/sec)
	HIA (%)	CaCo-2 (nm/sec)				
1	96.07	21.72	100	0.28	-2.80	4.91
2	96.32	21.67	100	0.30	-2.67	0.06
3	96.88	24.95	89.98	0.02	-2.98	2.76
4	97.26	28.69	90.57	0.12	-3.10	1.00

CaCo-2: CaCo-2 cell permeability; HIA: human intestinal absorption; PPB: plasma protein binding; BBB: blood-brain barrier penetration; SKIN: skin permeability; MDCK: Madin-Darby Canine Kidney cell permeability

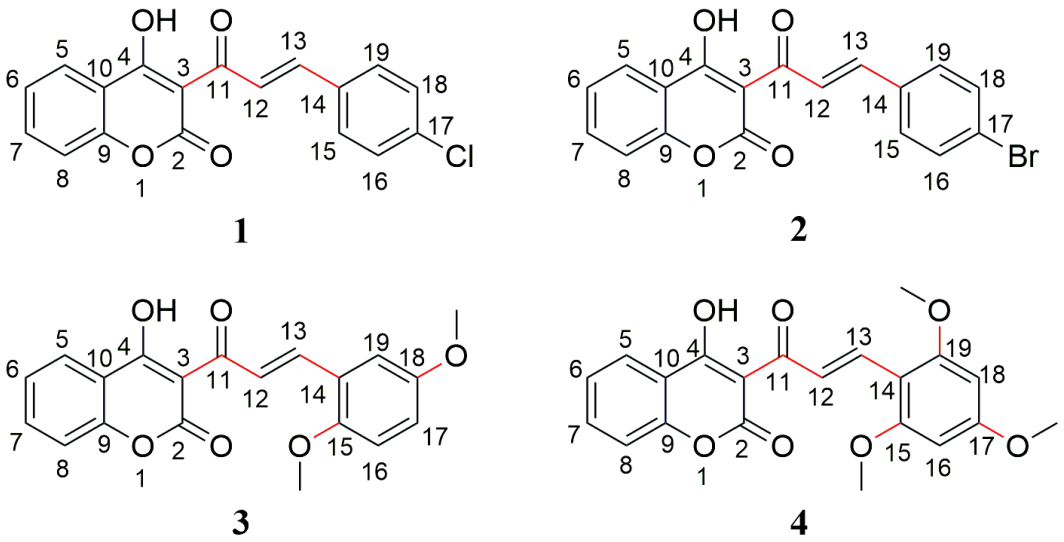

Figure 1.
Structures and rotatable bonds (in red) of compounds 1–4.

Permeability through the model of human colorectal carcinoma cells (CaCo-2) epithelial cells monolayers as well as Madin−Darby Canine Kidney cells (MDCK) is used for assessing the uptake efficiency of chemicals into the body [31] and to estimate the effect of the passage through the blood-brain barrier (BBB) [32, 33]. As these tests are time- and cost-intensive, we calculated them using computer programs. Human intestinal absorption (HIA) and plasma protein binding (PPB) are important for drug transport through the body [34]. Drugs with high protein binding tend to have a greater half-life compared to those with lower values. The greater the drug is bound to plasma protein, the less fraction of free drug is there for therapeutic effect [35]. Table II indicates that all four compounds were predicted to have high human intestinal absorption (> 96%) and high plasma protein binding (90 - 100%).

Permeability through the BBB is a precondition for compounds to show their potential effects on the central nervous system [36]. As observed from Table II, predicted *in vivo* blood-brain penetration for compound **3** was poor. On the other hand, compound **4**, which has one more methoxy group in the structure, was predicted to penetrate BBB at six times greater potency, whereas halogenated compounds were able to surpass the BBB with 15 times greater capacity in comparison to compound **3**. This is explained by the lowest TPSA values of compounds **1** and **2**.

For skin permeability (SKIN), many different *in silico* approaches predict the correlation between the structure of the permeants and their permeability, reproduce the skin behaviour and predict the ability of specific chemicals to permeate this barrier [37]. The predicted skin permeability for all compounds was poor.

Analysis of binding affinities of coumarin compounds

Molecular docking analysis on coumarin compounds showed significant binding affinities toward certain protein targets that have a critical function in the maintenance of DLBCL cell proliferation and survival (Table III) [38-40]. The results indicated that the compounds 2 and 3 formed the most significant complexes with unphosphorylated protein kinase B/Akt (PDB ID: 1GZO) with binding values lower than -10.00 kcal/mol. Protein kinase B (PKB), also known as Akt has an important role in tumour cell growth and survival. Upon Akt phosphorylation at Ser 473 and Thr 308 residues, activated protein translocates into the nucleus, promoting gene transcription that regulates cell cycle progression, protein synthesis, inhibition of apoptosis and many others [39, 41]. Compound 1 formed a strong complex with NF-κB/p52/RelB (PDB ID: 3DO7), with a very low dissociation constant. The expression of NF-κB transcription factor is prevalent in aggressive lymphoid malignancies, including DLBCL. Through regulation of gene expression, this transcription factor plays an important role in numerous biological processes, such as cell proliferation, differentiation, survival, growth and others [42]. Deregulation of the anti-apoptotic B-cell lymphoma 2 (BCL-2) protein family, including Mcl-1 is linked with lymphomagenesis and resistance to chemotherapeutic drugs. Mcl-1 promotes the progression survival of lymphoma cells by counteracting the activity of pro-apoptotic proteins [40]. Molecular docking data indicate that candidate compounds 2 and 1 form strong complexes with Mcl-1 protein (PDB ID: 6B4L), suggesting that the potential antitumor effect of the mentioned substances should be further evaluated.

Table III

Molecular docking parameters for coumarin derivatives with target proteins

Compound	Binding energy (kcal/mol)	Dissociation constant (μM)	Contacting amino acid residues (H-bonds)
Protein kinase B unphosphorylated (PDB ID: 1GZO)			
2	-10.32	0.027	Tyr 316
3	-10.27	0.030	Leu 278, Tyr 316
1	-9.10	0.212	-
4	-8.05	1.25	Lys 160, Lys 277, Asn 280, Gly 295
NF-κB p52/RelB (PDB ID: 3DO7)			
1	-9.98	0.048	His 62
2	-9.25	0.166	Arg 117
4	-9.06	0.228	Arg 117, Arg 119
3	-8.31	0.805	-
Mcl-1 (PDB ID: 6B4L)			
2	-9.76	0.070	-
1	-9.75	0.071	-
3	-9.63	0.088	-
4	-9.36	0.137	-

Evaluation of the antitumor potential of coumarin compounds in lymphoma cells

WST-8 assay was used to evaluate the effect of coumarin compounds on the metabolic activity of HBL-1 and DHL-4 cells that belong to ABC and GCB DLBCL subtypes, respectively. Compound **3** was insoluble in PBS and DMSO and it was excluded from further studies. The compounds have shown strong or no inhibitory activity (Figure 2) toward DLBCL cells. Compound **2** exerted strong inhibitory activity in HBL-1 cells that belong to the more aggressive subtype, where the percentage of viable cells decreased below 40% following the treatment with 50 μM concentration. Treatment with compounds **1** and **4** did not induce strong inhibitory activity, where the percentage of viable cells remained above 80% at the greatest treatment concentration (no inhibitory activity) in both cell lines. Interestingly, the cytotoxic effect of compound **2** varied among two DLBCL subtypes, indicating distinct mechanisms of action. While coumarin derivative induced strong inhibitory activity in HBL-1 cells, inhibitory activity was not observed in DHL-4 cells (Figure 2).

As compound **2** showed the most promising anti-tumour effect in the HBL-1 cell line, we evaluated the toxicity of the substance in the lung fibroblast MRC-5 cell line used as a control in this study (Figure 3).

Treatment with compound **2** did not show a strong cytotoxic effect in lung fibroblast cells (IC_{50} > 100.00 μM) which is one of the crucial factors in the development of new treatment options – cytotoxicity is achieved in cancer models without inhibitory effect in healthy cell lines. Although treatment of ABC DLBCL with compound 2 reduced cell viability by approx. 60% at the highest treatment concentration (50 μM), it is important to underline that in lung fibroblast cells strong toxicity was not observed even at two times greater concentration. Taking into consideration the low toxicity and sensitivity of healthy cells toward compound **2**, we further analysed the effect of the mentioned substance on cell death and protein expression in lymphoma cells.

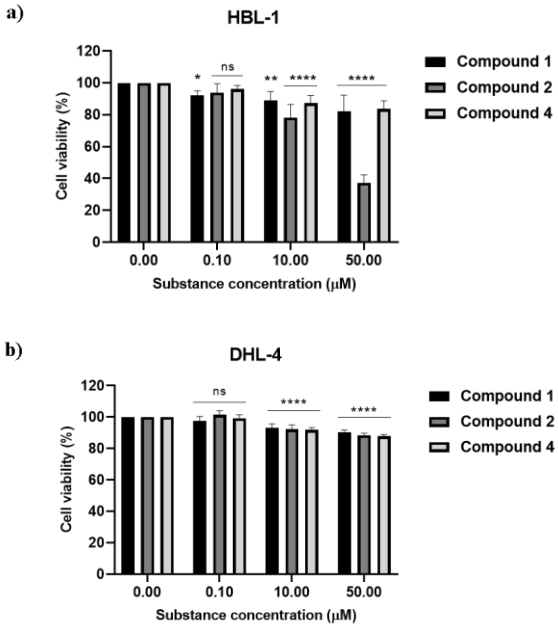

Figure 2.

Effects of compounds on cell viability after 48-hour incubation in HBL-1 (a) and DHL-4 (b) cell lines, as measured by WST-8 assay

Graphs represent the average of triplicates from three independent experiments with standard deviations indicated for each concentration. Cell viability is represented as a percentage compared to 0.05% DMSO control

$p < 0.05$ was considered as a level of statistical significance with the next levels: *$p < 0.05$, **$p < 0.01$, ***$p < 0.001$, ****$p < 0.0001$, ns – not significant

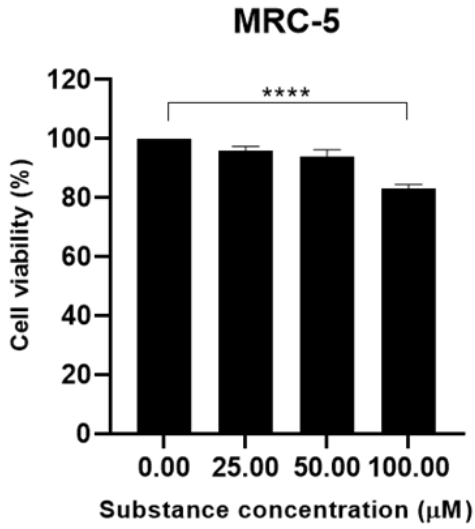

Figure 3.

Effect of compound 2 treatment on cell viability after 48-hour incubation in MRC-5 cell line, as measured by WST-8 assay

The graphs represent the average of triplicates from three repeated individual experiments with standard deviations indicated for each treatment. Cell viability is represented in percentage compared to the 0.1% DMSO control
$p < 0.05$ was considered as a level of statistical significance with the next levels: *$p < 0.05$, **$p < 0.01$, ***$p < 0.001$, ****$p < 0.0001$, ns – not significant

Using trypan blue assay, we assessed the effect of compound **2** which showed the most promising anti-tumour activity on cell death in DLBCL cells (Figure 4). Although we observed a strong cytotoxic effect of compound **2** in HBL-1 cells, trypan blue assay data showed no effect of the mentioned substance on cell death. Interestingly, compound **2** which previously showed no inhibitory activity toward DHL-4 cells exerted a greater effect on cell death compared to HBL-1 cells.

Our data suggest disparate activities of compound **2** in HBL-1 and DHL-4 cells in terms of cell metabolic activity and death. WST-8 assay represents a highly sensitive, non-toxic colorimetric assay where WST-8 tetrazolium salt is reduced to formazan dye by the activity of mitochondrial NAD(P)H enzymes [43]. Reversely, trypan blue dye is used for direct determination of the number of cells present in a sample. Live cells possess intact cell membranes that exclude the dye while the dye enters the dead cell as a result of compromised cell membranes where it binds intracellular proteins [44].

Cell-based assays represent essential tools for the preclinical evaluation of potential antitumor drug effects. A wide range of assays that target distinct cellular mechanisms have been used for antitumor drug evaluation in cells [45]. Therefore, in preclinical drug testing, it is important to apply different assay systems that operate through distinct mechanisms to understand the potential antitumor activity of the compound.

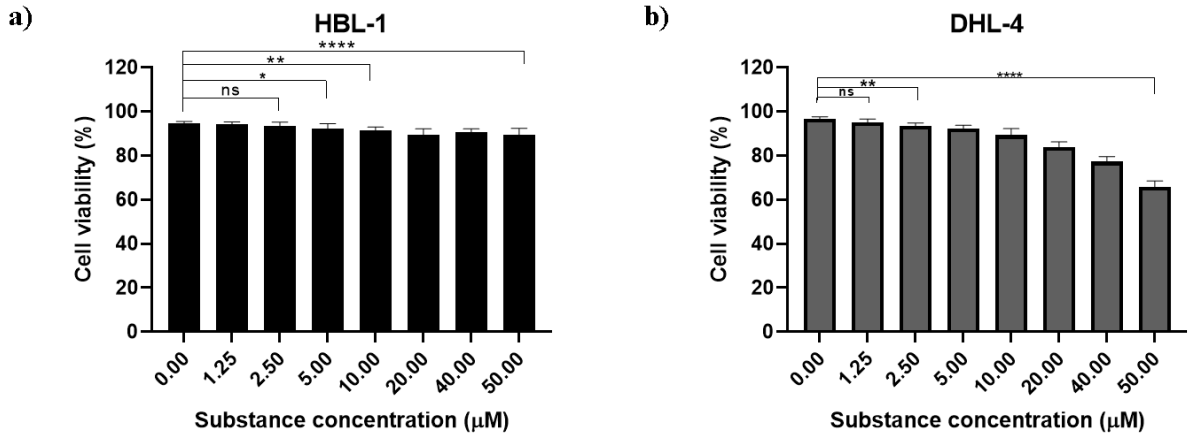

Figure 4.

Evaluation of cell death upon treatment with compound 2 in HBL-1 (a) and DHL-4 (b) cells, as measured by trypan blue assay

Each graph represents an average of triplicates from three independent experiments with standard deviations indicated for each concentration. Cell viability is represented in percentage compared to the 0.05% DMSO control
$p < 0.05$ was considered as a level of statistical significance with the next levels: *$p < 0.05$, **$p < 0.01$, ***$p < 0.001$, ****$p < 0.0001$, ns – not significant

Assessment of compounds' protein targets in DLBCL cells

Based on *in silico* and *in vitro* analysis results, we further evaluated the effect of compound **2** on protein targets that regulate cell proliferation and survival in HBL-1 and DHL-4 cells. The cells were treated with two concentrations of compounds (8 and 16 μM) for 48 hours (Figure 5).

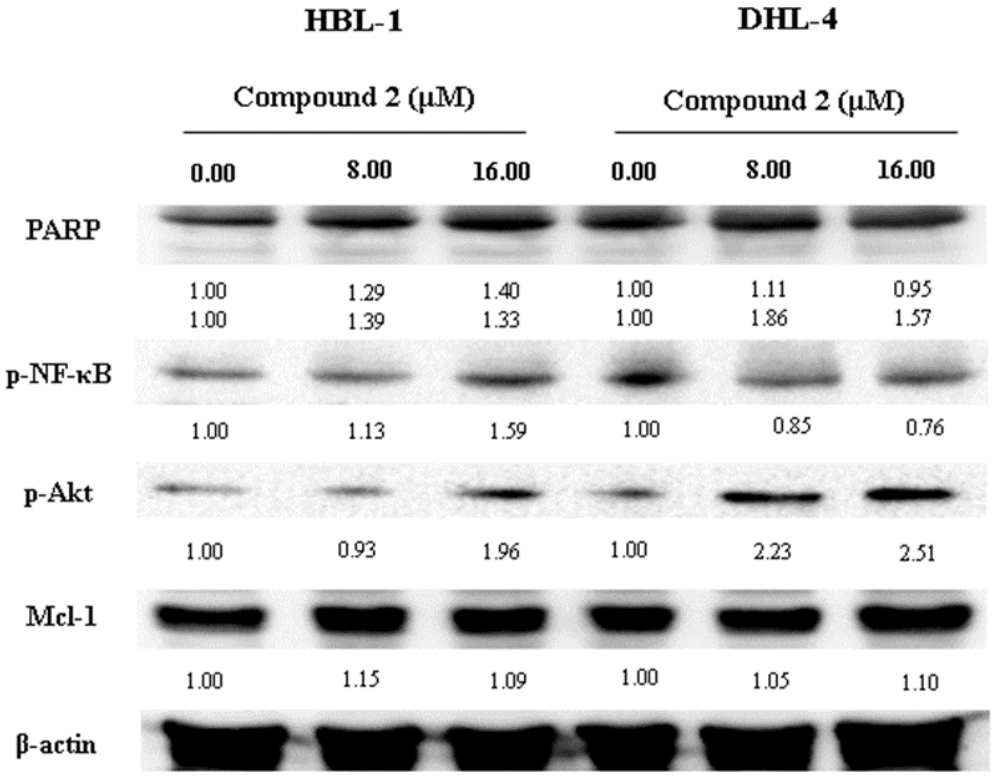

Figure 5.

Evaluation of protein expression following the treatment with compound **2** for 48 hours in HBL-1 and DHL-4 cells
Numbers below the bands represent a net image fold difference in the band intensity compared to the control and normalization against β-actin

The results of Western blot analysis indicate that the treatment with compound **2** at both treatment concentrations slightly stimulated the expression of PARP protein and its cleaved subunit. The expression of cleaved PARP protein was greater in DHL-4 cells. PARP family of members is recognized for their function of identification and repair of DNA double-stranded breaks through post-translational modifications by the addition of poly(ADP-ribose) chains [46]. Interestingly, compound **2** had opposing effects in terms of p-NF-κB expression in two cell lines. In HBL-1 cells, treatment with compound **2** resulted in a dose-dependent increase of phosphorylated NF-κB levels.

However, in DHL-4 cells, the expression of p-NF-κB protein decreased dose-dependently following the treatment with compound **2**. The expression of the target protein decreased by 24% compared to the control group at the higher treatment concentration. Interestingly, the expression of p-Akt was dose-dependently stimulated in both cell lines upon the treatment with compound **2**. More prominent expression of p-Akt was observed in DHL-4 cells where the expression levels of the target protein were increased to 2.5-fold at the highest treatment concentration in comparison to the untreated cells. Western blot analysis suggests that compound **2** did not have a significant effect on the expression of the Mcl-1 protein. In both cell lines, the expression of Mcl-1 was slightly induced. However, as these data represent a preliminary analysis, more experiments are required to understand the compound effect on the expression of the Mcl-1 protein.

One of the major characteristics of cancer cells is their ability to adapt to drug-response signalling processes that lead to therapeutic resistance [47, 48]. Such a phenomenon is achieved by different intra-cellular mechanisms, including alteration of drug targets, expression of detoxification mechanisms and drug pumps, increased DNA damage repair, apoptosis and many others [49]. Numerous reports suggest that drug administration can lead to the activation of compensatory mechanisms that reduce the activity of the drug [50]. PI3K/Akt/mTOR signalling pathway is commonly altered in human malignancies, including DLBCL [51, 52]. Constitutive activation of the PI3K/Akt signalling pathway as one of the main regulatory mechanisms for cancer cell survival and proliferation represents an important strategy for therapeutic approaches [47, 48, 53]. The activity of compensatory mechanisms that result in drug tolerance or resistance may be overcome by the application of combinatorial treatments that target distinct signalling pathways [50].

Even though activation of Akt signalling induces cell survival, numerous chemotherapeutic drugs stimulate Akt phosphorylation to achieve cellular therapeutic sensitivity [54]. Such a multimodality treatment approach suggests the application of PI3K/Akt inhibitors, including

MK-2206, that induce cancer cell sensitization to conventional therapy in *in vitro* and *in vivo* models [55]. Some of the chemotherapeutic drugs that are linked with induced phosphorylation of Akt in cancer cells include doxorubicin, 5-fluorouracil, gemcitabine, paclitaxel and others as a result of the activation of cell defence mechanisms that arise under stressful conditions [54, 56]. Overexpression of Akt is one of the potential mechanisms of cancer cell resistance to platinum therapy. Accordingly, increased levels of Akt in gastric cancer cells were reported as a major factor in the regulation of cisplatin resistance. The mechanism through which Akt triggered therapeutic resistance in these models was dependent on the activity of the Janus kinase 2 (JAK2) signalling pathway, suggesting that Akt represents a potential target for inhibition of cancer cell resistance to platinum-based therapy [57]. In another study, induced expression of Akt1 was linked with lung cancer cell resistance to cisplatin, where Akt1 inhibition resulted in the sensitivity of the cancer cell to the drug [58]. As previously mentioned, combinatorial treatment and application of Akt inhibitors could represent a promising mechanism to avoid therapeutic resistance in cells [50]. MK-2206, an Akt inhibitor showed a synergistic effect in combination with cisplatin in different tumour models, such as nasopharyngeal, gastric, lung and others, underlining the pivotal role of targeting Akt as a strategy to overcome chemo-resistance [55]. Combinatorial treatments are recognized as a promising strategy in the treatment of malignant disorders that are resistant to conventional therapy. This is achieved by the ability of drugs to target distinct signalling pathways to minimize drug resistance as cancer cells fail to adapt to the simultaneous cyto-toxic effects of two therapeutic agents [59]. Recently, the synergistic effect of metformin and thymoquinone in decreasing viability and proliferation of imatinib-sensitive and imatinib-resistant leukaemia cells was reported. The stronger synergistic effect of the two drugs was observed in cells resistant to imatinib therapy, indicating that the implication of combinatorial therapy that targets diverse cellular mechanisms in cancer models could offer a promising approach for cancer treatment in the future [60]. Moreover, osthole, a simple coumarin compound induced synergistic effect in combination with cisplatin, decreasing proliferation rate of human metastatic melanoma cells. On the contrary, furanocoumarins showed antagonistic effect in the same models [61]. Considering promising antitumor activity of coumarin derivatives in preclinical studies and clinical trials, it is noteworthy to evaluate the effect of compound **2** in combination with other anticancer drugs or Akt and NF-κB inhibitors that could potentially improve the treatment outcome. However, this remains to be evaluated in the future.

Conclusions

In the present research, compound **2** bearing bromine substituent showed strong cytotoxicity in HBL-1 cells, without inhibitory activity in the DHL-4 cell line. Treatment of both cell models stimulated the expression of p-Akt, while phosphorylated levels of NF-κB were decreased in DHL-4 cells. These data provide insight into the activation of compensatory mechanisms in DLBCL cells upon coumarin treatment. Considering the importance of combinatorial treatment approaches that increase therapeutic efficacy, we assume that the antitumor effect would be greater following the application of Akt inhibitors which remains to be evaluated in future experiments.

Acknowledgement

This work has been supported by the grant received from the Canton Sarajevo Ministry for Science, Higher Education and Youth, under the agreement number 27-02-35-37080-14/23 from 14.09.2023.

Conflict of interest

The authors declare no conflict of interest.

References

1. Sung H, Ferlay J, Siegel RL, Laversanne M, Soerjomataram I, Jemal A, Bray F, Global Cancer Statistics 2020: GLOBOCAN Estimates of Incidence and Mortality Worldwide for 36 Cancers in 185 Countries. *CA A Cancer J Clin.*, 2021; 71(3): 209-249.
2. Li S, Young KH, Medeiros LJ, Diffuse large B-Cell lymphoma. *Pathology*, 2018; 50(1): 74-87.
3. Sehn LH, Salles G, Diffuse Large B-Cell Lymphoma. *N Engl J Med.*, 2021; 384(9): 842-858.
4. Meng X, Min Q, Wang JY, B cell lymphoma. B Cells in Immunity and Tolerance, Wang JY, Ed.; Springer: Singapore, Singapore, 2020; 1254; 161-181.
5. Alizadeh AA, Eisen MB, Davis RE, Ma C, Lossos IS, Rosenwald A, Boldrick JC, Sabet H, Tran T, Yu X, Powell JI, Yang L, Marti GE, Moore T, Hudson JJr, Lu L, Lewis DB, Tibshirani R, Sherlock G, Chan WC, Greiner TC, Weisenburger DD, Armitage JO, Warnke R, Levy R, Wilson W, Grever RG, Byrd JC, Botstein D, Brown PO, Staudt LM, Distinct types of diffuse large B-cell lymphoma identified by gene expression profiling. *Nature*, 2000; 403(6769): 503–511.
6. Cioroianu AI, Stinga PI, Sticlaru L, Cioplea MD, Nichita L, Popp C, Tumor Microenvironment in Diffuse Large B-Cell Lymphoma: Role and Prognosis. *Anal Cell Pathol (Amst.)*, 2019; 2019: 8586354.
7. Davis RE, Ngo VN, Lenz G, Tolar P, Young RM, Romesser PB, Kohlhammer H, Lamy L, Zhao H, Yang Y, Xu W, Shaffer AL, Wright G, Xiao W, Powell J, Jiang JK, Thomas CJ, Rosenwald A, Ott G, Muller-Hermelink HK, Gascoyne RD, Connors JM, Johnson NA, Rimsza LM, Campo E, Jaffe ES, Wilson WH, Delabie J, Smeland EB, Fisher RI, Braziel RM, Tubbs RR, Cook JR, Weisenburger

DD, Chan WC, Pierce SK, Staudt LM, Chronic active B-cell-receptor signalling in diffuse large B-cell lymphoma. *Nature*, 2010; 463(7277): 88-92.
8. Basso K, Klein U, Niu H, Stolovitzky GA, Tu Y, Califano A, Cattoretti G, Dalla-Favera R, Tracking CD40 signaling during germinal center development. *Blood*, 2004; 104(13): 4088-4096.
9. Epperla N, Hamadani M, Hematopoietic cell transplantation for diffuse large B-cell and follicular lymphoma: Current controversies and advances. *Hematol Oncol Stem Cell Ther*., 2017; 10(4): 277-284.
10. Špirtović-Halilović S, Salihović M, Džudžević-Čančar H, Trifunović S, Roca S, Softić D, Završnik D, DFT study and microbiology of some coumarin-based compounds containing a chalcone moiety. *J Serb Chem Soc.*, 2014; 79(4): 435-443.
11. Špirtović-Halilović S, Salihović M, Trifunović S, Roca S, Veljović E, Osmanović A, Vinković M, Završnik D, Density functional theory: 1H and 13C-NMR spectra of some coumarin derivatives. *J Serb Chem Soc.*, 2014; 79(11): 1405-1411.
12. Sashidhara KV, Kumar A, Kumar M, Sarkar J, Sinha S, Synthesis and *in vitro* evaluation of novel coumarin–chalcone hybrids as potential anticancer agents. *Bioorg Med Chem Lett.*, 2010; 20(24): 7205-7211.
13. Srikrishna D, Godugu C, Dubey PK, A Review on Pharmacological Properties of Coumarins. *Mini Rev Med Chem.*, 2018; 18(2): 113-141.
14. Stefanachi A, Leonetti F, Pisani L, Catto M, Carotti A, Coumarin: A Natural, Privileged and Versatile Scaffold for Bioactive Compounds. *Molecules*, 2018; 23(2): 250.
15. Venugopala KN, Rashmi V, Odhav B, Review on natural coumarin lead compounds for their pharmacological activity. *BioMed Res Int.*, 2013; 2013: 963248.
16. Završnik D, Špirtović-Halilović S, Softić D, Synthesis, structure and antibacterial activity of 3-substituted derivatives of 4-hydroxycoumarin. *Period Biol.*, 2011; 113(1): 93-97.
17. Završnik D, Bašić F, Bečić F, Bečić E, Jažić S, Synthesis, structure and biological activity of 3-substituted derivatives of 4-hydroxycoumarin. *Period Biol.*, 2003; 105(2): 137-139.
18. Klosa J, Simple method for the preparation of ketones of 4-hydroxycoumarin with the aid of phosphorus oxychloride. *Arch Pharm Ber Dtsch Pharm Ges.*, 1955; 288(8-9): 356-361, (available in German).
19. Daina A, Michielin O, Zoete V, ILOGP: a simple, robust, and efficient description of n -octanol/water partition coefficient for drug design using the GB/SA approach. *J Chem Inf Model.*, 2014; 54(12): 3284-3301.
20. Daina A, Michielin O, Zoete V, SwissADME: a free web tool to evaluate pharmacokinetics, drug-likeness and medicinal chemistry friendliness of small molecules. *Sci Rep.*, 2017; 7: 42717.
21. Krieger E, Vriend G, New ways to boost molecular dynamics simulations. *J Comput Chem.*, 2015; 36(13): 996-1007.
22. Krieger E, Vriend G, YASARA View—molecular graphics for all devices—from smartphones to workstations. *Bioinformatics*, 2014; 30(20): 2981-2982.
23. Morris GM, Huey R, Lindstrom W, Sanner MF, Belew RK, Goodsell DS, Olson AJ, AutoDock4 and AutoDockTools4: Automated docking with selective receptor flexibility. *J Comput Chem.*, 2009; 30(16): 2785-2791.
24. Duan Y, Wu C, Chowdhury S, Lee MC, Xiong G, Zhang W, Yang R, Cieplak P, Luo R, Lee T, Caldwell J, Wang J, Kollman P, A point-charge force field for molecular mechanics simulations of proteins based on condensed-phase quantum mechanical calculations. *J Comput Chem.*, 2003; 24(16): 1999-2012.
25. Schnur DM, Grieshaber MV, Bowen JP, Development of an internal searching algorithm for parameterization of the MM2/MM3 force fields. *J Comput Chem.*, 1991; 12(7): 844-849.
26. Dudek MJ, Ponder JW, Accurate modeling of the intramolecular electrostatic energy of proteins. *J Comput Chem.*, 1995; 16(7): 791-816.
27. Norberg E, Lako A, Chen PH, Stanley IA, Zhou F, Ficarro SB, Chapuy B, Chen L, Rodig S, Shin D, Choi DW, Lee S, Shipp MA, Marto JA, Danial NN, Differential contribution of the mitochondrial translation pathway to the survival of diffuse large b-cell lymphoma subsets. *Cell Death Differ.*, 2017; 24(2): 251-262.
28. Lipinski CA, Lombardo F, Dominy BW, Feeney PJ, Experimental and computational approaches to estimate solubility and permeability in drug discovery and development settings. *Adv Drug Delivery Rev.*, 2001; 46(1-3): 3-26.
29. Veber DF, Johnson SR, Cheng HY, Smith BR, Ward KW, Kopple KD, Molecular properties that influence the oral bioavailability of drug candidates. *J Med Chem.*, 2002; 45(12): 2615-2623.
30. Congreve M, Carr R, Murray C, Jhoti H, A "rule of three" for fragment-based lead discovery?. *Drug Discov Today*, 2003; 8(19): 876-877.
31. Artursson P, Palm K, Luthman K, Caco-2 monolayers in experimental and theoretical predictions of drug transport. *Adv Drug Deliv Rev.*, 2001; 46(1-3): 27-43.
32. Summerfield SG, Read K, Begley DJ, Obradović T, Hidalgo IJ, Coggon S, Lewis AV, Porter RA, Jeffrey P, Central nervous system drug disposition: the relationship between *in situ* brain permeability and brain free fraction. *J Pharmacol Exp Ther.*, 2007; 322(1): 205-213.
33. Hubatsch I, Ragnarsson EGE, Artursson P, Determination of drug permeability and prediction of drug absorption in Caco-2 monolayers. *Nat Protoc.*, 2007; 2(9): 2111-2119.
34. Yan A, Wang Z, Cai Z, Prediction of human intestinal absorption by GA feature selection and support vector machine regression. *Int J Mol Sci.*, 2008; 9(10): 1961-1976.
35. Ghafourian T, Amin Z, QSAR models for the prediction of plasma protein binding. *BioImpacts*, 2013; 3(1): 21-27.
36. Daneman R, Prat A, The blood–brain barrier. *Cold Spring Harb Perspect Biol.*, 2015; 7(1): a020412.
37. Pecoraro B, Tutone M, Hoffman E, Hutter V, Almerico AM, Traynor M, Predicting Skin Permeability by Means of Computational Approaches: Reliability and Caveats in Pharmaceutical Studies. *J Chem Inf Model.*, 2019; 59(5): 1759-1771.
38. Kloo B, Nagel D, Pfeifer M, Grau M, Düwel M, Vincendeau M, Dörken B, Lenz P, Lenz G,

Krappmann D, Critical role of PI3K signaling for NF-kappaB–dependent survival in a subset of activated B-cell–like diffuse large B-cell lymphoma cells. *Proc Natl Acad Sci USA*, 2011; 108(1): 272-277.
39. Wang J, Xu-Monette ZY, Jabbar KJ, Shen Q, Manyam GC, Tzankov A, Visco C, Wang J, Montes-Moreno S, Dybkær K, Tam W, Bhagat G, Hsi ED, van Krieken JH, Ponzoni M, Ferreri AJM, Wang S, Møller MB, Piris MA, Medeiros LJ, Li Y, Pham LV, Young KH, AKT Hyperactivation and the Potential of AKT-Targeted Therapy in Diffuse Large B-Cell Lymphoma. *Am J Pathol.*, 2017; 187(8): 1700-1716.
40. Wang MY, Li T, Ren Y, Shah BD, Lwin T, Gao J, Shain KH, Zhang W, Zhao X, Tao J, MCL-1 dependency as a novel vulnerability for aggressive B cell lymphomas. *Blood Cancer J.*, 2021; 11(1): 14.
41. Zhang R, Chen M, Yu L, Jin Z, Anticancer activity of diphenhydramine against pancreatic cancer by stimulating cell cycle arrest, apoptosis, and modulation of PI3K/Akt/mTOR pathway. *Farmacia*, 2021; 69(5): 967-973.
42. Kennedy R, Klein U, Aberrant Activation of NF-kB Signalling in Aggressive Lymphoid Malignancies. *Cells*, 2018; 7(11): 189.
43. Chamchoy K, Pakotiprapha D, Pumirat P, Leartsakulpanich U, Boonyuen U, Application of WST-8 based colorimetric NAD(P)H detection for quantitative dehydrogenase assays. *BMC Biochem.*, 2019; 20(1): 4.
44. Strober W, Trypan blue exclusion test of cell viability. *Curr Protoc Immunol.*, 2019; 111: A3.B.1-A3.B.3.
45. Kumar N, Afjei R, Massoud TF, Paulmurugan R, Comparison of cell-based assays to quantify treatment effects of anticancer drugs identifies a new application for Bodipy-L-cystine to measure apoptosis. *Sci Rep.*, 2018; 8(1): 16363.
46. Franzese O, Graziani G, Role of PARP Inhibitors in Cancer Immunotherapy: Potential Friends to Immune Activating Molecules and Foes to Immune Checkpoints. *Cancers (Basel)*, 2022; 14(22): 5633.
47. Logue JS, Morrison DK, Complexity in the signaling network: insights from the use of targeted inhibitors in cancer therapy. *Genes Dev.*, 2012; 26(7): 641-650.
48. Trusolino L, Bertotti A, Compensatory pathways in oncogenic kinase signaling and resistance to targeted therapies: six degrees of separation. *Cancer Discov.*, 2012; 2(10): 876-880.
49. Cree IA, Charlton P, Molecular chess? Hallmarks of anti-cancer drug resistance. *BMC Cancer*, 2017; 17(1): 10.
50. Ilan Y, Overcoming Compensatory Mechanisms toward Chronic Drug Administration to Ensure Long-Term, Sustainable Beneficial Effects. *Mol Ther Methods Clin Dev.*, 2020; 18: 335-344.
51. Yuan C, Liu Y, Hao Y, Yan L, Jliang J, Jin H, Mechanism of rituximab in the treatment of neuromyelitis optica. *Farmacia*, 2022; 70(4): 636-642.
52. Bergholz JS, Zhao JJ, How Compensatory Mechanisms and Adaptive Rewiring Have Shaped Our Understanding of Therapeutic Resistance in Cancer. *Cancer Res.*, 2021; 81(24): 6074-6077.
53. von Manstein V, Yang CM, Richter D, Delis N, Vafaizadeh V, Groner B, Resistance of Cancer Cells to Targeted Therapies Through the Activation of Compensating Signaling Loops. *Curr Signal Transduct Ther.*, 2013; 8(3): 193-202.
54. Li X, Lu Y, Liang K, Liu B, Fan Z, Differential responses to doxorubicin-induced phosphorylation and activation of Akt in human breast cancer cells. *Breast Cancer Res.*, 2005; 7(5): R589-597.
55. Avan A, Narayan R, Giovannetti E, Peters GJ, Role of Akt signaling in resistance to DNA-targeted therapy. *World J Clin Oncol.*, 2016; 7(5): 352-369.
56. Alvarez-Tejado M, Naranjo-Suárez S, Jiménez C, Carrera AC, Landázuri MO, del Peso L, Hypoxia induces the activation of the phosphatidylinositol 3-kinase/Akt cell survival pathway in PC12 cells. *J Biol Chem.*, 2001; 276(25): 22368-22374.
57. Zhang LL, Zhang J, Shen L, Xu XM, Yu HG, Overexpression of AKT decreases the chemosensitivity of gastric cancer cells to cisplatin *in vitro* and *in vivo*. *Mol Med Rep.*, 2013; 7(5): 1387-1390.
58. Liu LZ, Zhou XD, Qian G, Shi X, Fang J, Jiang BH, AKT1 amplification regulates cisplatin resistance in human lung cancer cells through the mammalian target of rapamycin/P70S6K1 pathway. *Cancer Res.*, 2007; 67(13): 6325-6332.
59. Bayat Mokhtari R, Homayouni TS, Baluch N, Morgatskaya E, Kumar S, Das B, Yeger H, Combination therapy in combating cancer. *Oncotarget*, 2017; 8(23): 38022-38043.
60. Glamočlija U, Mahmutović L, Bilajac E, Šoljić V, Vukojević K, Suljagić M, Metformin and Thymoquinone Synergistically Inhibit Proliferation of Imatinib-Resistant Human Leukemic Cells. *Front Pharmacol.*, 2022; 13: 867133.